Soils and Rocks
An International Journal of Geotechnical and Geoenvironmental Engineering
www.soilsandrocks.com
ISSN 1980-9743
ISSN-e 2675-5475

Comparative evaluation of constitutive models for stress-strain analysis of an iron ore tailings from the *Quadrilátero Ferrífero*, Minas Gerais, Brazil

André de Oliveira Faria[1#], Bruno Guimarães Delgado[1,2,3], Lucas Deleon Ferreira[1], Mauro Pio dos Santos Junior[4]

Article

Keywords
Critical state soil mechanics
Modified Cam-Clay
NorSand

Abstract

The study and understanding of the concepts related to critical state soil mechanics is relatively recent in Brazil, especially among practicing geotechnical engineers in the mining industry, where simpler solutions were traditionally adopted. This raises the necessity to develop studies capable of promoting discussions about the benefits of the approaches from the critical state theory. In this context, this research aims to evaluate the behavior of an iron ore tailings from the *Quadrilátero Ferrífero* through critical state computational models, considering the Modified Cam-Clay and NorSand model. The numerical results from the use of the models simulated the ductile/brittle behavior of the material in drained shear and it was observed that for loose samples both models produced similar results. The simulations in undrained shear, on the other hand, highlighted the differences between the models, with the NorSand showing a strength loss in undrained shear (strain-softening) whereas the Modified Cam-Clay Model exhibited a ductile behavior. In general, the NorSand model was the one that presented the best numerical response in relation to the experimental behavior, which may be linked to the use of the largest number of parameters, to the concept that particulate materials exist in a set of states and the silty characteristic of the material. Additionally, it was observed the difficulty to simulate the dense behavior of materials with the model, which may be associated with the formation of 'shear bands' during the experimental test and the complexity of modeling the occurrence of this phenomenon in virtual tests using the NorSand model.

1. Introduction

The stress-strain behavior of the soils is not an element dissociated from its resistance and vice versa. The correlation between deformability and resistance is associated through a tridimensional yield surface that involves q, p', e, represented through mathematical equations described in elastoplastic models, in which the deformations can be treated in elastic and plastic domains separately. In this aspect, the critical state soil mechanics (CSSM) proposes an integrated approach for these themes by introducing the critical state concept.

Casagrande (1936) evaluated the behavior of sands in loose and dense states through direct shear tests in drained conditions and noticed that loose sands tend to contract when shared, whereas dense sands tend to exhibit a dilatant behavior under shear. At large strains, Casagrande (1975) observed that the materials presented the same void ratio, classified as the critical void ratio (e_c).

Taylor (1948) observed that the critical void ratio is affected by the mean effective stress (p'), becoming smaller with the increasing of the confining stress. The author evaluated the soil behavior during the plastic phase and observed that the relationship between the final void ratio and the logarithm of the applied stress can be given as a straight line parallel and slightly inferior to the normal compression line (NCL), classified as the ultimate condition of the material and named as the critical state line (CSL).

[1]Universidade Federal de Ouro Preto, Ouro Preto, MG, Brasil.
[2]Vale, Geotechnical Directorate, Belo Horizonte, MG, Brasil.
[3]Universidade do Porto, Faculdade de Engenharia, Construct-Geo, Porto, Portugal.
[4]Pimenta de Ávila Consultoria, Belo Horizonte, MG, Brasil.
[#]Corresponding author. E-mail address: ofaria.andre@gmail.com

Submitted on October 19, 2022; Final Acceptance on September 8, 2023; Discussion open until May 31, 2024.
https://doi.org/10.28927/SR.2024.011022

In the 1960s, Gonzalo Castro (1969) undertook a series of stress-controlled triaxial tests in uniform, clean quartz sand (Banding Sand) in order to create the flow structure envisioned by Arthur Casagrande. These tests were able to demonstrate the strain-softening on loose samples under undrained shear, leading to the *steady state* condition.

Poulos (1981) formalized the definition of the *steady state* as "the state in which the mass is continuously deforming at constant volume, constant normal effective stress, constant shear stress and constant velocity". In this context, the locus of steady-state void rations with mean effective stress was referred to as the *steady-state* locus (SSL).

Been et al. (1991) examined the difference between the critical and steady-state lines and concluded that, for practical purposes, equivalence could be assumed.

The representation of the CSL on the $q - p'$ and $e - p'$ planes can be represented by Equation 1 and 2, respectively.

$$q = Mp' \tag{1}$$

$$e_c = \Gamma - \lambda \ln\left(p_c^{'}\right) \tag{2}$$

where q is the deviator stress, M is the critical friction ratio, Γ is the 'altitude' of CSL defined at 1 kPa, λ is the slope of CSL and $p_c^{'}$ is the critical mean effective stress.

Additionally, through triaxial compression tests, M can be determined according to Equation 3.

$$M = \frac{6\sin\varphi_c^{'}}{3 - \sin\varphi_c^{'}} \tag{3}$$

where $\varphi_c^{'}$ is the effective friction angle at the critical state.

Studies related to the behavior of mining tailings from the perspective of CSSM are recent (Smith et al., 2019; Torres-Cruz & Santamarina, 2020; Paes & Cirone, 2021; Silva et al., 2022; Viana da Fonseca et al., 2022), which makes the knowledge about the behavior of these materials still restricted.

This paper is the outcome of a research developed to characterize the behavior of an iron ore tailings from the *Quadrilátero Ferrífero* (Minas Gerais state, Brazil) through numerical modeling, using Modified Cam-Clay and NorSand model, and to compare the results with the stress-strain behavior observed experimentally in triaxial compression tests. It is also the objective of this paper to promote a discussion about the need to use the concepts of CSSM in stress-strain studies, in addition to simplified solutions such as those using the Mohr-Coulomb yield surface equation, especially in the mining industry.

2. Materials and methods

The data used in the research came from the campaign of tests carried out at LabGeo (*Laboratório de Geotecnia*, written in Portuguese) located at FEUP (*Faculdade de Engenharia da Universidade do Porto*, written in Portuguese), presented in the research of Eloi (2021) and reinterpreted for the present study. The author discussed about conventional and advanced laboratory procedures to determine critical state parameters of an ore tailings, from triaxial compression tests under drained conditions.

The geotechnical characterization of the tailings was conducted by performing i) grain size analysis (LNEC, 1966); ii) test for specific gravity of soil solids (G_s) according to the Portuguese Standard NP-83 (IGPAI, 1965); iii) one-dimensional consolidation test and iv) drained triaxial compression tests under confining pressures of 100, 200 and 400 kPa. According to Eloi (2021), the tests to determine the Atterberg limits defined the material as non-plastic and were omitted from the research.

The numerical modeling was performed by the Finite Element Method (FEM) in the SIGMA/W module of the GeoStudio 2021.3 software to represent the experimental behavior of the material under axisymmetric compression.

2.1 Geotechnical characterization

The particle size distribution (PSD) curve, determined according to D422-63 (ASTM, 2007), is indicated in Figure 1. As can be seen, the tailings composition is, on average, 8.1% of fine sand, 83.6% of silt-sized particles and 8.3% of clay-sized particles.

The specific gravity (G_s) was defined as 4.55 and the results obtained from the one-dimensional consolidation test are given in Figure 2.

The results from the one-dimensional consolidation test indicate a steeper slope of the NCL from the initial condition of the test up to stress values close to 12 kPa, which, according to Eloi (2021), is associated with the sample preparation method (moist tamping) of the specimen. Increasing the stress above this point there is a decrease in the slope of the NCL and a pronounced tendency of linearity up to stress values close to 800 kPa, from which point there is a subtle increase in the slope of the line, which according to the author can be explained by the additional generation of fines in the specimen during the test (grain crushing). The results of the NCL slope (λ) and the slope of the recompression/expansion line (k), obtained from the oedometer test, are presented in Table 1.

The drained triaxial compression tests were performed with the tailings in a loose state (CID-01, CID-02 and CID-04) and dense state (CID-03). The CID-03 test presented inconsistencies in the stress-strain response and was only used to define the parameters related to the dilation phenomenon of the NorSand model. Therefore, only the CID-01, CID-02 and CID-04 tests were used to determine the drained strength parameters of the material, using the maximum deviatoric stress criterion ($c' = 0$ kPa and $\varphi' = 35.4°$).

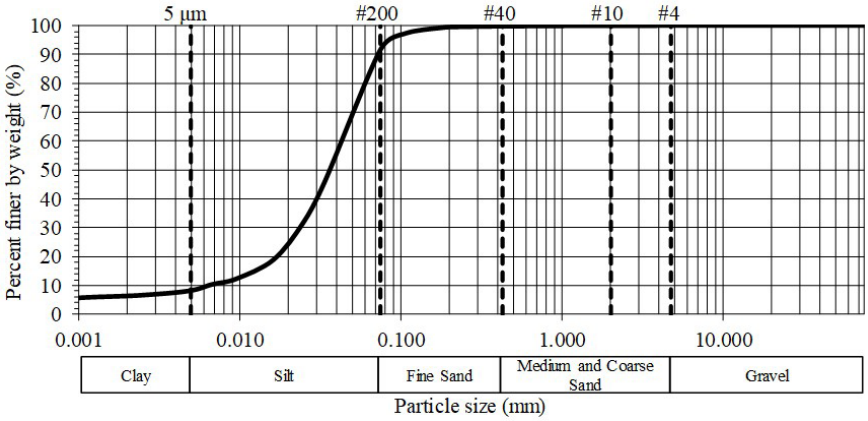

Figure 1. PSD curve of the silt tailings according to the standard D422-63 (ASTM, 2007) (from Eloi, 2021).

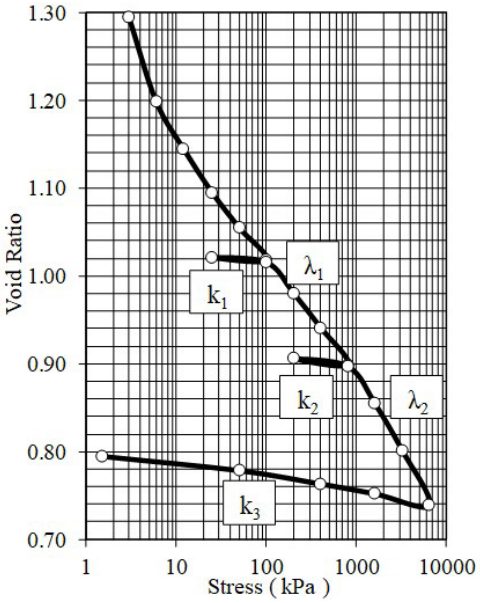

Figure 2. Virgin curve and recompression curve obtained from the oedometer test (from Eloi, 2021).

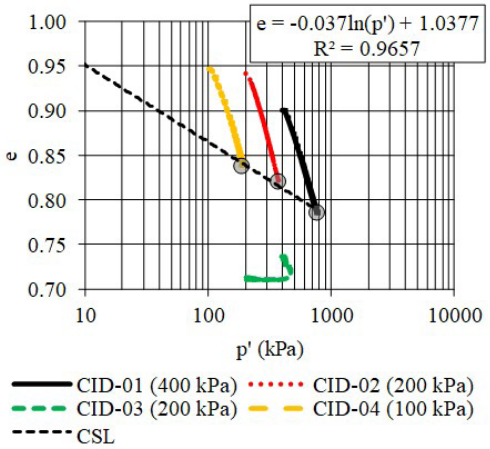

Figure 3. CSL on the $e - p'$ plane (from Eloi, 2021).

Using the same idea applied to the definition of the drained strength parameters, the CSL was defined from the CID-01, CID-02 and CID-04 tests, at the critical state condition. The CSL on the $e - p'$ plane is shown in Figure 3.

According to Figure 3, the CID-03 test did not reach the critical state, which can be explained by the possible formation of preferential 'shear bands' due to the dense condition of the material during the test. The critical state parameters (λ and Γ) were defined as 0.037 and 1.038, respectively. The CSL in the $q - p'$ plane is shown in Figure 4.

As can be seen in Figure 4, it was possible to define the critical friction ratio (M) as equal to 1.397. Additionally, using Equation 3, the value of the effective friction angle in the critical state (φ_c') is equal to 34.5°.

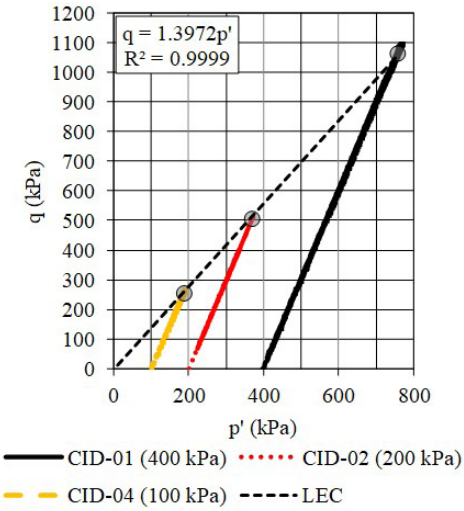

Figure 4. Projection of the critical state line on the $q - p'$ plane (from Eloi, 2021).

Table 1. Values for λ e *k*.

Region	Parameter	Value
Virgin Curve (compression)	λ_1	0.059
	λ_2	0.076
Rebound Curve (decompression)	k_1	0.002
	k_2	0.005
	k_3	0.007
Recompression	$_1$	0.004
	k_2	0.006

Table 2. Modified Cam-Clay model parameters.

Parameters	CID-01	CID-02	CID-03	CID-04
e_0	0.90	0.94	0.71	0.95
γ (kN/m³)	28.12	27.73	30.13	27.69
OCR	1	1	6	1
λ	0.076			
k	0.004			
v	0.10			
$\varphi_c^{'}$ (°)	34.5			
M	1.397			

2.2 Constitutive models

2.2.1 Modified Cam-Clay

The proposition of the Cam-Clay model was possible through the evolution of the initial studies of Roscoe et al. (1958), evolving from the concept of critical state supported by experimental evidence and the concepts of the plasticity theory by Drucker et al. (1957), until its final description by Schofield & Wroth (1968) and later modified by Roscoe & Burland (1968), when it was referenced as Modified Cam-Clay model.

Classified as the first model to consider the CSSM, Roscoe et al. (1958) defined that a feature of the soil (particulate material) when subjected to a shear distortion, is that it eventually reaches a critical state condition capable of continuing the distortion without further change in void ratio. The initial model explains the behavior of loose materials without considering the occurrence of cementation due to the clay mineral particles. According to Roscoe & Burland (1968), the model explains the mechanical behavior of samples with clayey behavior, normally to slightly overconsolidated (*OCR* ≤ 2.72), which exhibits a contractive behavior during shear.

After the original model definition, the possibility of increments occurrence of plastic distortional strain was observed for increments of p' in the condition of stress ratio $\eta = 0$ (where $\eta = q / p'$), which is classified as an inconsistency of the model, considering that the occurrence of distortional deformations must be associated with the application of distortional stress (q). Additionally, according to Roscoe & Burland (1968), the equations proposed by the model initially overestimated the values of strain increment for the initial stages of the triaxial compression tests (low values of η), as well as the model overestimated the values of coefficient of earth pressure at rest (K_0). In this aspect, Roscoe & Burland (1968) proposes a new yield surface, in order to correct such points observed in the original model.

The shape of the yield surface for the Modified Cam-Clay model consists in an ellipse described by Equation 4, such that the yield surface will be characterized by an ellipsoid in the principal stress space.

$$\frac{p'}{p_y^{'}} = \frac{M^2}{M^2 + \eta^2} \tag{4}$$

where $p_y^{'}$ is the mean effective stress on the yield surface.

Equation 4 describes a set of ellipses, all of them with the same shape, controlled by M, passing through the origin and with its dimension defined by $p_y^{'}$. As in the original model, the Modified Cam-Clay assumes that the yield surface expands isotropically.

The Modified Cam-Clay modeling parameters are shown in Table 2. The normal consolidation condition (*OCR* = 1) was used for the tests with the loose material (CID-01, CID-02 and CID-04) and overconsolidation (*OCR* = 6) for the test with dense material, in order to simulate the dilation effect. Additionally, for the compressibility parameters, the value of λ corresponding to the high-stress levels (above 800 kPa in Figure 2) was adopted for the virgin curve (compression) and for the rebound curve (decompression) the average of the values presented in Table 1 was adopted for the parameter k, given the better convergence in the numerical model.

2.2.2 NorSand

Such as the Modified Cam-Clay, the NorSand model is also based on the CSSM. The model was developed during the 1980s and 1990s, based on the experience with the construction of structures on loose sands. The analysis of the occurrence of static liquefaction during the construction of these structures contributed to the development of the model, initially proposed by Jefferies (1993) and later by Jefferies & Been (2016).

Therefore, as the names suggest, the intent of the model is to describe the behavior of loose and dense sands, in both drained and undrained conditions, in order to better represent experimentally observed behavior in these materials. In this aspect, it can predict with good approximation behavior of static liquefaction and dilatant behavior.

Differently from the models that consider the existence of a single NCL parallel to the CSL, as in the Cam-Clay models, the NorSand model introduces the concept of infinite NCL that differ according to the initial void ratio of the soil and its deformation history, intercepting the CSL.

Given this pattern of numerous NCLs, Jefferies & Been (2016) consider it is necessary to use two parameters to characterize the soil state: i) the state parameter (Ψ), responsible for measuring the individual location of each NCL on the $e - p'$ plane; and ii) the overconsolidation ratio (OCR), which measures the proximity of the material state in relation to the NCL, when evaluated on the p' axis. In this aspect, the NorSand model classifies as the first model to consider the state parameter within the CSSM approach.

Been & Jefferies (1985) defined that the state parameter represents the distance of the current void ratio of the soil in comparison to the critical void ratio for the same mean stress, as described by Equation 5. Thus, this distance, or state path, can be used to indicate the soil behavior and its tendency of volumetric deformation during shear.

$$\Psi = e - e_c \tag{5}$$

where negative values of Ψ are representative of dilatant materials under drained shear and positive values are indicative of contractive soils.

From the evaluation of a set of triaxial compression tests performed on sand-like soils with different fines contents, Jefferies & Been (2016) suggest a unique relation between the state parameter (Ψ) and the maximum dilatancy (which is D_{min} because of the compression positive convention), according to Equation 6.

$$D_{min} = \chi_{tc}\Psi \tag{6}$$

where χ_{tc} (state-dilatancy) is a soil property defined under drained triaxial compression tests and D_{min} generally occurs at the peak stress ratio (i.e. $\eta_{máx}$). From the CID-03 test, with the material initially in dense condition, it was possible to define the state-dilatancy according to Figure 5.

The yield surface of the NorSand is given by Equation 7, which uses the same principle of the Cam-Clay models.

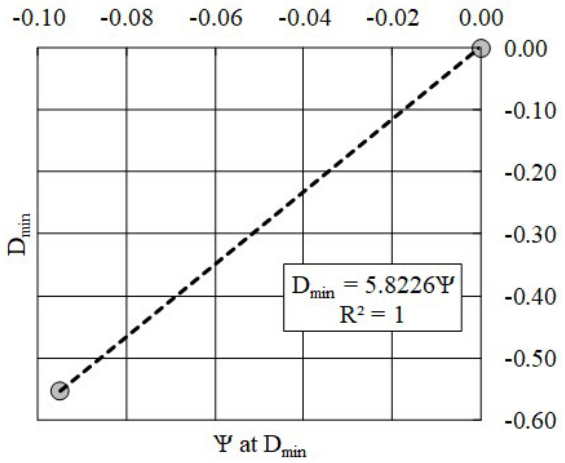

Figure 5. Parameter χ definition.

$$\eta = M_i\left[1 - \ln\left(\frac{p}{p_i}\right)\right] \tag{7}$$

where the subscript "i" represents the image condition.

Jefferies & Been (2016) defines the image condition as a transient condition of the material, in which the volumetric strain rate changes from contractile to dilatant. Ishihara et al. (1975) called this transient condition the phase transformation and others have called it the pseudo-steady state.

The yield surface of the NorSand model differs from the Cam-Clay models due to the consideration of the image condition concept. Furthermore, the mean stress at the image state (p_i) describes the yield surface size, in the same way that in the Cam-Clay models the yield surface size is associated with CSL. Additionally, the NorSand considers that the material can present plastic strains anywhere on the $e - p'$ plane, so that there is no 'elastic wall' confining the plastic behavior, as in the Cam-Clay models.

About the plasticity parameters of the model, the volumetric coupling coefficient from Nova's flow rule (N) can be defined by Equation 8 (Jefferies & Shuttle, 2002).

$$\eta_{máx} = M_{tc} - (1 - N)D_{min} \tag{8}$$

From the CID-03 test with the material initially in dense condition, it was possible to define the parameter N, according to Figure 6.

The plastic hardening modulus (H), which is a plastic hardening parameter in NorSand, was calibrated with the process Iterative Forward Modeling (IFM) proposed by Jefferies & Been (2016) according to Equation 9.

$$H = H_0 - H_y\Psi \tag{9}$$

where H_0 is the modulus for the condition of state parameter equal to zero and H_y represents the modulus as a function of the state parameter. The H relation in Equation 9 provides a good fit with $H_0 = 184.5$ and $H_y = 1{,}666$, according to Figure 7.

The parameters used for the modeling with the NorSand model are shown in Table 3.

The elastic shear modulus (G) was defined according to the best calibration obtained during the analysis, since tests with bender elements, specific radial instrumentation or resonant column tests were not carried out, which would allow greater assertiveness in the definition of this parameter.

3. Analysis and results

3.1 Modified Cam-Clay results

The results obtained using the Modified Cam-Clay to calibrate the laboratory tests can be seen in Figure 8, where the axial strain (ε_a) is shown on the x-axis and the deviator stress (q) is shown on the y-axis, and Figure 9, where

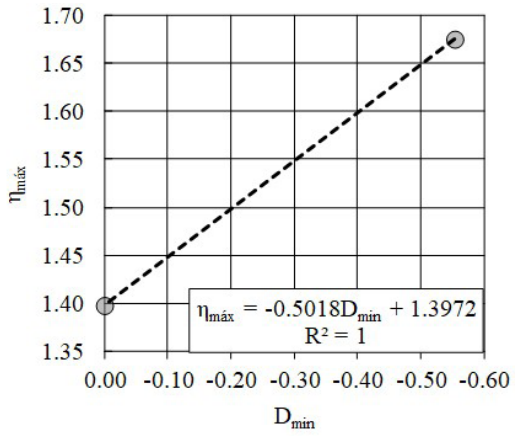

Figure 6. Parameter N definition.

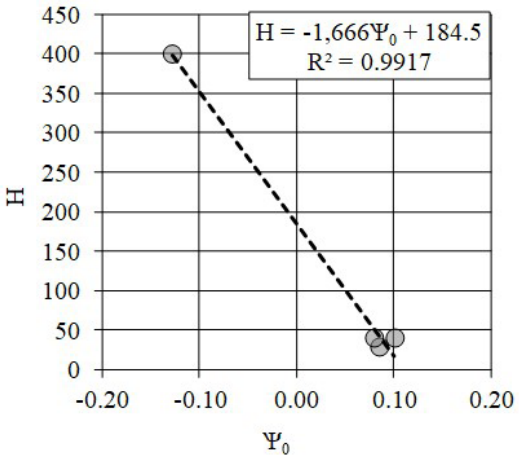

Figure 7. Relation between H and Ψ_0 with IFM method.

Table 3. NorSand model parameters.

Parameters	CID-01	CID-02	CID-03	CID-04
e_0	0.90	0.94	0.71	0.95
γ (kN/m³)	28.12	27.73	30.13	27.69
OCR	1			
Ψ_0	0.08	0.10	-0.12	0.08
ν	0.10			
G_{ref} (MPa)	50			
m	0.50			
p'_{ref} (kPa)	100			
Γ	1.037			
λ	0.037			
M	1.397			
N	0.498			
χ	5.822			
H	30	40	400	40
H_0	184.5			
H_y	1.666			

the x-axis represents the axial strain (ε_a) and the y-axis represents the volumetric strain (ε_v). These figures compare the experimental tests (loose samples: CID-01, CID-02 and CID-04; dense sample: CID-03) with the numerical results.

As can be seen in Figure 8 and Figure 9, the numerical analysis was able to capture either the ductile (for loose samples – CID-01, CID-02 and CID-04) or brittle behavior (for the dense sample – CID-03) of the tailings, showing a good convergence between the analysis and experimental tests. The results for the volumetric strain in the numerical model with loose tailings were slightly lower than the experimental behavior, showing a higher difference for the CID-01 and CID-02 tests.

Figure 8 shows that the numerical model was able to represent the loss of strength observed in the CID-03 (dense tailings) for lower strains (brittle behavior), with the model indicating a higher loss of strength than the experimental response. The dilatant behavior of the CID-03 test was simulated with good approximation until axial strains close to 5%. In order to obtain a good fit with the experimental result, the condition of $OCR = 6$ was used for this sample. Such consideration occurs because the model uses the OCR to simulate the dilatancy effect, just as the NorSand model uses the state parameter (Ψ) to represent this phenomenon. The adoption of a high OCR value is because the Modified Cam-Clay model is better applicable for normally consolidated clayey materials, which is different from the silty material in dense condition used in the present research.

In terms of void ratio variation, as can be seen in Figure 10, the results obtained by the numerical model were satisfactory, except for the variation near LEC, in which the model slightly underestimated the critical void ratio, especially for the CID-02 test.

3.2 NorSand results

The results obtained using the NorSand model to calibrate the laboratory tests are shown in Figure 11 and Figure 12. Just as in Section 3.1, these figures show the comparison between the experimental tests (loose samples: CID-01, CID-02 and CID-04; dense sample: CID-03) and the numerical results.

As can be seen in Figure 11 the stress-strain numerical results were able to capture the experimental behavior, especially for CID-02, CID-04 and CID-03. This figure also indicates that the CID-01 numerical results were the most divergent from the experimental behavior. Just as in Modified Cam-Clay, the NorSand model was able to simulate the ductile and brittle behavior of the material. The volumetric strain response (Figure 12) for loose materials (CID-01, CID-02 and CID-04) obtained in the numerical model was slightly lower than the experimental results, with the sample CID-01 showing higher divergence, which could be adjusted with the better determination of the elastic shear modulus (G) through laboratory tests.

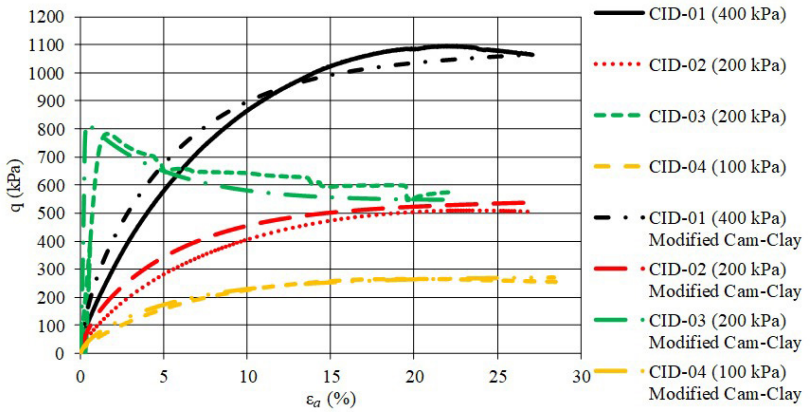

Figure 8. Stress-strain – Modified Cam-Clay model.

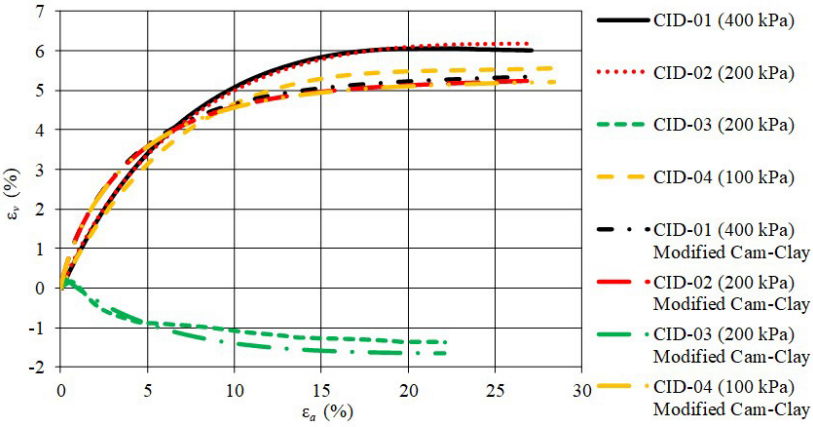

Figure 9. Strain paths – Modified Cam-Clay model.

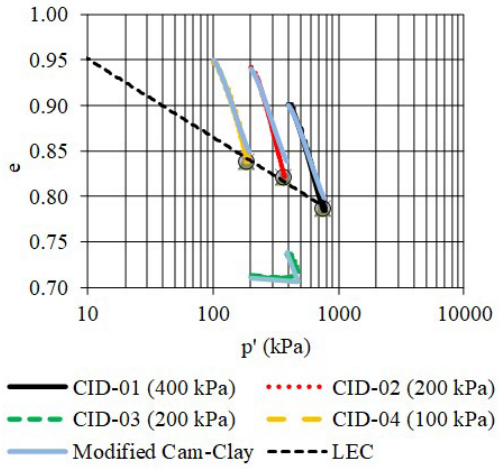

Figure 10. Void ratio variation – Modified Cam-Clay model.

The CID-03 stress-strain modeling result was considerably close to the experimental behavior, properly simulating the loss of strength at low deformations (brittle behavior) and the variation of the deviator stress with axial strain during the test. Additionally, with the NorSand modeling was possible to get a greater convergence with the pre-peak stress-strain curves, which preserves a greater adherence in terms of brittle behavior in comparison with experimental data.

The NorSand model was able to simulate the experimental volumetric strain until the peak deviator stress for the CID-03 test, just as observed by Silva et al. (2022). However, the post-peak volumetric strain was not a good convergence from CID-03. According to Silva et al. (2022), this divergence may be associated with the formation of 'shear bands' (a phenomenon that occurs only in very dense samples), and limitations of the boundary conditions defined in the modeling, given the complexity of modeling the occurrence of this phenomenon in virtual tests using the NorSand model. In this context, it was observed that the volumetric strains were mostly influenced by the state-dilatancy (χ) during the modeling, so that the decrease in the values of this parameter tends to decrease the volumetric strain, as shown in Figure 13.

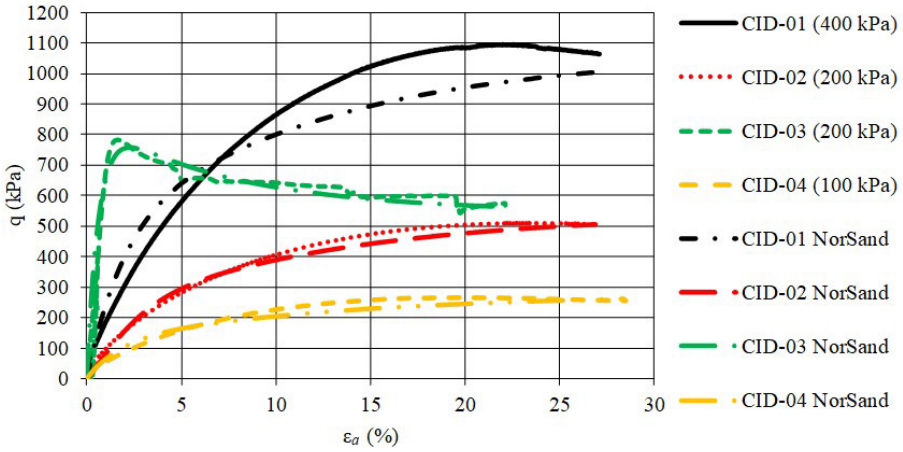

Figure 11. Stress-strain – NorSand model.

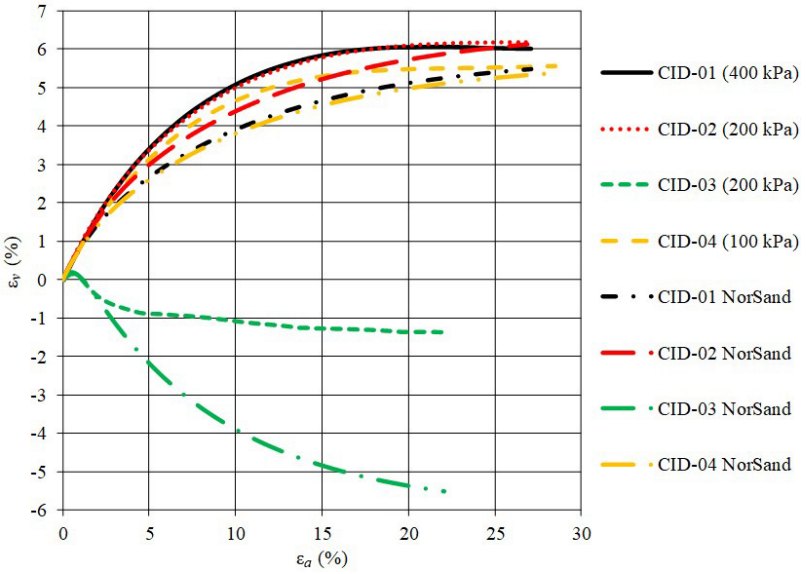

Figure 12. Strain paths – NorSand model.

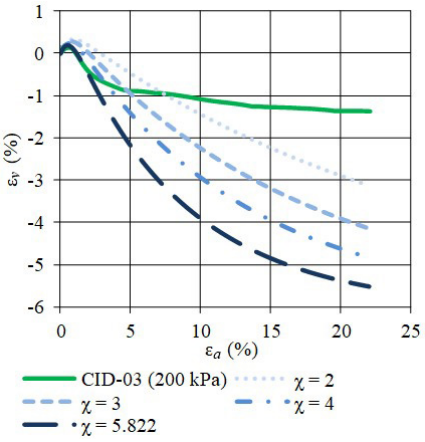

Figure 13. Sensibility evaluation of state-dilatancy (χ).

It was evident that high values of this parameter (χ) result in a relevant decoupling of the post-peak volumetric strains. This aspect reinforces the need for carrying out very careful tests to seek greater assertiveness in the definition of this parameter, aiming to use the NorSand model or other more sophisticated constitutive models. A reference in terms of laboratory care can be obtained by Viana da Fonseca et al. (2021).

Regarding the void ratio variation, as well as in the Modified Cam-Clay, the NorSand model was able to reproduce the experimental behavior for loose samples (CID-01, CID-02 and CID-04), as shown in Figure 14. For the CID-03 test (dense sample), the model also reproduced the experimental behavior and extended the void ratio variation to the LEC, which was not observed in the Modified Cam-Clay.

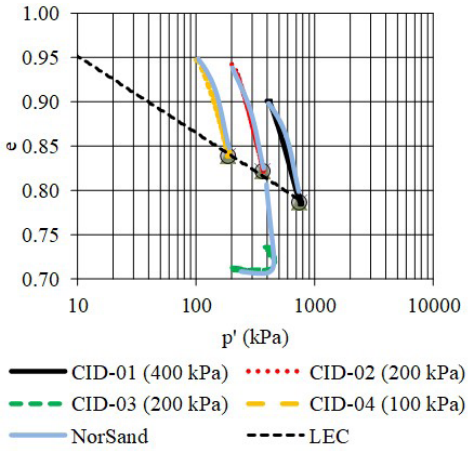

Figure 14. Void ratio variation – NorSand model.

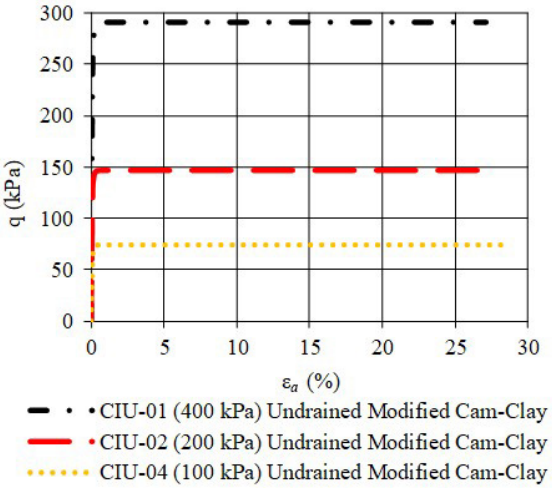

Figure 15. Stress-strain Modified Cam-Clay model – Undrained condition.

3.3 Undrained performance

In order to evaluate the difference between the two models in terms of undrained behavior, the Cam-Clay and NorSand parameters given in Table 2 and 3, respectively, were used to numerically simulate a series of undrained triaxial compression tests under confining pressures of 100, 200 and 400 kPa (similar to the confining pressures performed for the tests CID-01, CID-02 and CID-04). For this condition, this study was not able to compare the results with experimental data, given that the data base used in this research did not have undrained triaxial compression test.

As can be seen in Figures 15 and 16, there is a considerable difference between the models in terms of loss of strength in undrained shear. While the NorSand model simulated the abrupt strength loss at low strains (brittle behavior), which is characteristic of flow liquefaction, the Modified Cam-Clay model showed a ductile behavior, which is characteristic of normally consolidated clayey materials.

It was observed a higher stiffness in the Modified Cam-Clay model, compared to the NorSand. Such response can be associated with the low value of the *k* parameter (slope of recompression/expansion line), given the silty nature of the material. Since that parameter describes the elastic response of the model, the stiffness tends to decrease as its values increase. Figure 17 shows the sensibility evaluation for the *k* parameter.

Despite the observation of the model's similarity for the tests considering loose samples under drained conditions, these two models showed highly different behavior when the simulation was performed in undrained conditions. Thus, it is possible to notice that the NorSand model captures the typical behavior of flow liquefaction (strain-softening under undrained shear), whereas the Modified Cam-Clay is not able to model such behavior.

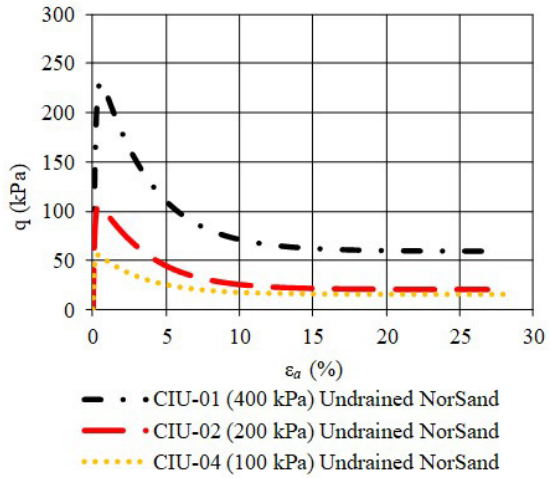

Figure 16. Stress-strain NorSand model – Undrained condition.

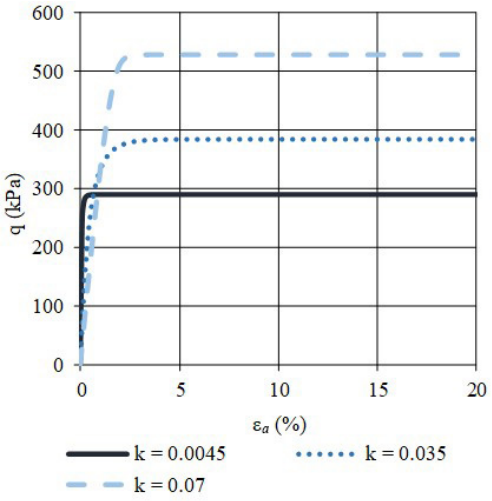

Figure 17. Sensibility evaluation for the *k* parameter.

4. Conclusion

This study evaluated the behavior of an iron ore tailings from the *Quadrilátero Ferrífero* (Minas Gerais state, Brazil) using numerical models to calibrate experimental triaxial compression tests performed on a silt tailings. The calibration was performed using the Modified Cam-Clay and NorSand model. Additionally, characterization of the tailings was presented to describe the material.

The Modified Cam-Clay model was able to simulate the ductile/brittle behavior of the tailings in drained condition. To simulate the behavior of the CID-03 test (dense condition) the adoption of $OCR = 6$ was necessary, in order to reproduce its volumetric strain in drained condition and its dilatancy.

In terms of numerical response, the NorSand model simulated the ductile/brittle behavior of the loose material in the same manner as the Modified Cam-Clay. For the simulation of the material behavior in dense condition (CID-03 test), the modeling resulted in considerably higher volumetric strains compared to the experimental test, which may be associated with the formation of 'shear bands' and limitations of the boundary conditions defined in the NorSand modeling, just as observed by Silva et al. (2022). This illustrates the need for greater understanding in terms of constitutive modeling to better represent the dense behavior of materials, eventually through the development of more representative models and careful tests.

It was observed that for loose samples (CID-01, CID-02 e CID-04) the drained models produced similar results. In this case, to model the dense condition different approaches were used to simulate the dilatancy of the soil: i) using the consideration of $OCR = 6$ for the Modified Cam-Clay model and ii) using a negative state parameter (Ψ) for NorSand ($\Psi < -0.05$). Additionally, for the modeling in undrained condition, the simulation of the abrupt strength loss at low strains (characteristic of flow liquefaction) was observed in the NorSand model, whereas the Modified Cam-Clay yielded a ductile behavior, which is expected from more clay-like soils.

Understanding the state in terms of the state parameter for this tailings is believed to be the most appropriate given its nature (silt-sized and non-plastic tailings), which is the reason to believe that the Nor-Sand model would be the better critical state constitutive model to capture its behavior, especially because the fact that the model was able to simulate the strength loss at low strains (brittle behavior) in undrained shear, observed in recent failures of tailings dams with silty materials in the *Quadrilátero Ferrífero* (Minas Gerais state, Brazil).

The difficulty in using the state-dilatancy (χ) was highlighted, since it was defined from the use of only one triaxial test. A higher quantity of tests in dense condition can provide a better calibration of this parameter. Additionally, it was noted the need to perform laboratory tests to provide more precision in the determination of the elastic shear modulus (G), since this parameter has a significant influence on the convergence during the modeling. Finally, there is a need for further study about the formation of 'shear bands' for samples in dense condition, with the adoption of very careful practices and very specific laboratory implements (Viana da Fonseca et al., 2021), given the complexity of modeling this phenomenon with NorSand and that they are not yet in current use in Geotechnical Laboratories, notably in Brazil.

Despite the differences between the models, the responses obtained with the Modified Cam-Clay and NorSand are good evidence to illustrate the importance of considering the concepts of the CSSM in stress-strain studies. This finding reinforces the need for greater dedication to research and studies related to this topic, encouraging the application of such methods in project and consulting companies operating in the mining industry, namely in the process of evaluating tailings disposal structures, for which the more simplified models and approaches might not be sufficient to capture its more sophisticated behavior.

Acknowledgements

The authors would like to acknowledge the CAPES (*Coordenação de Aperfeiçoamento de Pessoal de Nível Superior*, written in Portuguese) and the Graduate Program in Geotechnics of School of Mines Geotechnics Center (NUGEO) at the Federal University of Ouro Preto (UFOP).

Declaration of interest

The authors have no conflicts of interest to declare. All co-authors have observed and affirmed the contents of the paper and there is no financial interest to report.

Authors' contributions

André de Oliveira Faria: conceptualization, data curation, visualization, writing – original draft. Bruno Guimarães Delgado: methodology, formal analysis, writing – review & editing. Lucas Deleon Ferreira: supervision, resources, validation. Mauro Pio dos Santos Junior: formal analysis, validation.

Data availability

The datasets generated and analyzed in the course of the current study are available from the corresponding author upon request.

List of symbols

c'	Effective cohesion intercept
e	Void ratio
e_0	Initial void ratio
e_c	Critical void ratio

k	Slope of recompression/expansion line
m	Elastic shear modulus power coefficient
p'	Mean effective stress
p'_{ref}	Mean effective stress (usually defined equal 100 kPa)
p_c	Critical mean stress
p'_c	Critical mean effective stress
	Mean stress at image condition
p'_y	Mean effective stress on the yield
q	Deviator stress
CID	Drained Isotopically Consolidated
CSL	Critical State Line
D_{min}	Maximum dilatancy
E'	Effective Young's modulus
G	Elastic shear modulus
G_s	Specific gravity
G_{ref}	Elastic shear modulus on a reference mean effective stress of 100 kPa
H	Plastic hardening modulus
H_0	Plastic hardening modulus for the condition of state parameter equal to zero
H_y	Plastic hardening modulus as a function of the state parameter
IFM	Interactive Forward Modeling
K_0	Coefficient of earth pressure at rest
M	Critical friction ratio
M_{tc}	Critical friction ratio obtained by the triaxial compression test
M_i	Critical friction ratio at image condition
N	Volumetric coupling coefficient
NCL	Normal Compression Line
OCR	Overconsolidation Ratio
γ	Total unit weight
ε_a	Axial strain
ε_v	Volumetric strain
ε_s	Shear strain
η	Stress ratio
$\eta_{máx}$	Maximum stress ratio
λ	Slope of CSL on $e - p'$ plane
λ	Slope of NCL
σ'	Effective normal stress
σ_1	Major principal stress
σ_3	Minor principal stress
τ	Mhear stress
ν	Poisson's ratio
φ'	Effective friction angle
φ'_c	Effective friction angle at the critical state
χ , χ_{tc}	State-dilatancy
ψ	Dilation angle
Γ	'Altitude' of CSL defined at 1 kPa
Ψ	State parameter
Ψ_0	State parameter at the start of shearing

References

ASTM D422-63. (2007). *Standard test method for particle-size analysis of soils*. ASTM International, West Conshohocken, PA. http://dx.doi.org/10.1520/D0422-63R07E01.

Been, K., & Jefferies, M.G. (1985). A state parameter for sands. *Geotechnique*, 35(2), 99-112. http://dx.doi.org/10.1680/geot.1985.35.2.99.

Been, K., Jefferies, M.G., & Hachey, J. (1991). The critical state of sands. *Geotechnique*, 41(3), 365-381. http://dx.doi.org/10.1680/geot.1991.41.3.365.

Casagrande, A. (1936). Characteristics of cohesionless soils affecting the stability of slopes and earth fills. *Journal of Boston Society of Civil Engineers*, 23, 257-276.

Casagrande, A. (1975). Liquefaction and cyclic deformation of sands: a critical review. In *Proceedings of the 5th Pan-American Conference on Soil Mechanics and Foundation Engineering* (pp. 79-133). Buenos Aires, Argentina.

Castro, G. (1969). *Liquefaction of sands* [PhD thesis, Harvard University]. Cambridge, MA: Harvard University.

Drucker, D.C., Gibson, R.E., & Henkel, D.J. (1957). Soil mechanics and work-hardening theories of plasticity. *Transactions of the American Society of Civil Engineers*, 122(1), 338-346. http://dx.doi.org/10.1061/TACEAT.0007430.

Eloi, D.M. (2021). Ensaios triaxiais com procedimentos convencionais e avançados para avaliação de estados críticos [MSc dissertation, Universidade do Porto]. Universidade do Porto's repository (in Portuguese). Retrieved in October 19, 2022, from https://hdl.handle.net/10216/133473

Inspeção Geral dos Produtos Agrícolas e Industriais – IGPAI. (1965). *NP-83: determinação da densidade das partículas*. Lisboa: IGPAI (in Portuguese).

Ishihara, K., Tatsuoka, F., & Yasuda, S. (1975). Undrained deformation and liquefaction of sand under cyclic stresses. *Soil and Foundation*, 15(1), 29-44. http://dx.doi.org/10.3208/sandf1972.15.29.

Jefferies, M. (1993). Nor-Sand: a simple critical state model for sand. *Geotechnique*, 43(1), 91-103. http://dx.doi.org/10.1680/geot.1993.43.1.91.

Jefferies, M., & Been, K. (2016). *Soil liquefaction: a critical state approach* (2nd ed.). Boca Raton: CRC Press.

Jefferies, M., & Shuttle, D.A. (2002). Dilatancy in general Cambridge-type models. *Geotechnique*, 52(9), 625-638. http://dx.doi.org/10.1680/geot.2002.52.9.625.

Laboratório Nacional de Engenharia Civil – LNEC. (1966). *LNEC E 196: solos: análise granulométrica*. Lisboa: LNEC (in Portuguese).

Paes, I., & Cirone, A. (2021). Geotechnical characterization of a silty phosphate ore tailing within critical state theory geotechnical modelling of CPR grouting view project. In *Proceedings of the 7th International Conference on Tailings Management* (pp. 1-10). Gecamin.

Poulos, S.J. (1981). The steady state of deformation. *Journal of the Geotechnical Engineering Division*, 107(5), 553-562. http://dx.doi.org/10.1061/AJGEB6.0001129.

Roscoe, K.H., & Burland, J.B. (1968). On the generalized stress-strain behavior of "wet" clay. In J. Heyman & F. Leckie (Eds.), *Engineering plasticity* (pp. 535-608). Cambridge: Cambridge University Press.

Roscoe, K.H., Schofield, A.N., & Wroth, C.P. (1958). On the yielding of soils. *Geotechnique*, 8(1), 22-53. http://dx.doi.org/10.1680/geot.1958.8.1.22.

Schofield, A., & Wroth, P. (1968). *Critical state soil mechanics.* New York: McGraw-Hill.

Silva, J.P.S., Cacciari, P.P., Torres, V.F.N., Ribeiro, L.F.M., & Assis, A.P. (2022). Behavioural analysis of iron ore tailings through critical state soil mechanics. *Soils and Rocks*, 45(2), 1-13. http://dx.doi.org/10.28927/SR.2022.071921.

Smith, K., Fanni, R., Chapman, P., & Reid, D. (2019). Critical state testing of tailings: comparison between various tailings and implications for design. In *Proceedings of the Tailings and Mine Waste* (pp. 1183-1195). Vancouver: University of British Columbia.

Taylor, D.W. (1948). *Fundamentals of soil mechanics.* New York: John Wiley & Sons.

Torres-Cruz, L.A., & Santamarina, J.C. (2020). The critical state line of nonplastic tailings. *Canadian Geotechnical Journal*, 57(10), 1508-1517. http://dx.doi.org/10.1139/cgj-2019-0019.

Viana da Fonseca, A., Cordeiro, D., & Molina-Gómez, F. (2021). Recommended procedures to assess critical state locus from triaxial tests in cohesionless remoulded samples. *Geotechnics*, 1(1), 95-127. http://dx.doi.org/10.3390/geotechnics1010006.

Viana da Fonseca, A., Cordeiro, D., Molina-Gómez, F., Besenzon, D., Fonseca, A., & Ferreira, C. (2022). The mechanics of iron tailings from laboratory tests on reconstituted samples collected in post-mortem Dam I in Brumadinho. *Soils and Rocks*, 45(2), 1-20. http://dx.doi.org/10.28927/SR.2022.001122.